

## Supporting Information

### **In Situ Fabrication of Plasmonic Bi@Bi<sub>2</sub>O<sub>2</sub>CO<sub>3</sub> Core-Shell Heterostructure for Photocatalytic CO<sub>2</sub> Reduction: Structural Insights into Selectivity Modulation**

Yannan Zhou,<sup>a</sup> Jingyun Jiang,<sup>b</sup> Hang Yin,<sup>\*a</sup> and Shouren Zhang<sup>\*a</sup>

<sup>a</sup> Henan Provincial Key Laboratory of Nanocomposites and Applications, Institute of Nanostructured Functional Materials, Huanghe Science and Technology College, Zhengzhou 450006, China

E-mail addresses: hangyin@hhstu.edu.cn

<sup>b</sup> School of Materials Science and Engineering, Zhengzhou University, Zhengzhou 450052, P.R. China

\*Corresponding author.

#### **Experimental Procedures**

**Materials:** Polyethylene glycol (PEG) 200 and barbituric acid (BA) were purchased from Sinopharm Chemical Reagent Co., Ltd. Bismuth nitrate pentahydrate (Bi(NO<sub>3</sub>)<sub>3</sub>·5H<sub>2</sub>O) were obtained from Shanghai Aladdin Biochemical Technology Co., Ltd. Nafion solution (5%) was purchased from DuPont Corp. Deionized water obtained from a Milli-Q ultrapure water purification system was used in all experiments.

**Characterization.** The morphology and microstructure of the samples were examined by emission scanning electron microscope (SEM, Quanta 250) and transmission electron microscopes (TEM, FEI Tecnai Spirit 12). High-resolution transmission electron microscopy (HRTEM), scanning transmission electron microscopy (STEM), and elemental mapping images were acquired on an FEI Tecnai F20 microscope with an acceleration voltage of 200 kV. The X-Ray diffraction (XRD) patterns were collected at room temperature on a Bruker D8, irradiated with monochromatic Cu K $\alpha$  radiation. The X-ray photoelectron spectroscopy (XPS) was recorded with PHI5000 Versaprobe (Japan) with an Al K $\alpha$  X-ray source. Electron paramagnetic resonance (EPR) spectra were conducted by a Bruker EMXplus at the room

temperature. UV/Vis diffuse reflectance spectra were measured on a Hitachi U-4100 ultraviolet/visible/NIR spectrophotometer. Photoluminescence (PL) spectra were recorded on a F-4600 spectrofluorometer with the excitation wavenumber of 310 nm at room temperature. The fluorescence lifetime was determined by recording the time-resolved fluorescence emission spectra on a fluorescence spectrophotometer (Edinburgh Instruments, FLSP-920). The secondary cutoff binding energy was measured by AXIS SUPRA X-ray photoelectron spectroscopy with He I as the excitation source. An HP 5973 GC-mass spectrometer was employed to analyze the  $^{13}\text{CO}$  generated from the  $^{13}\text{CO}_2$  isotopic experiment.

**Catalysts preparation.**  $\text{Bi}@\text{Bi}_2\text{O}_2\text{CO}_3$  heterostructures were synthesized via a one-step solvothermal process under carefully controlled reaction media. The large-sized Bi sphere with the ultrathin  $\text{Bi}_2\text{O}_2\text{CO}_3$  layer epitaxially grown in situ ( $\text{Bi}@\text{Bi}_2\text{O}_2\text{CO}_3$ ) was obtained in the synthesized DESs, which were composed by mixing polyethylene glycol (PEG 200) with barbituric acid (BA) at molar ratios of 16:1. In a typical process, 10 mmol  $\text{Bi}(\text{NO}_3)_3 \cdot 5\text{H}_2\text{O}$  was dissolved in 30 mL DES under continuous magnetic stirring. The solutions were then transferred to Teflon-lined autoclave and heated in an oven at 200 °C for 12 h. After the autoclave cooled, the products were collected by centrifugation, washed several times with water and ethanol, and dried at 60 °C for 2 h in the oven. The obtained samples were designated as DES Bi. The small Bi nanospheres aggregated into the  $\text{Bi}_2\text{O}_2\text{CO}_3$  nanosheets ( $\text{Bi}/\text{Bi}_2\text{O}_2\text{CO}_3$ ), hydrothermally prepared in pure PEG 200 at 200 °C for 12 h were designated as PEG Bi.

**Photocatalytic  $\text{CO}_2$  reduction reaction.** Photocatalytic  $\text{CO}_2$  reduction experiments were conducted in an H-shaped gas-tight quartz reactor separated by Nafion®212 membrane. Circulating water was pumped to maintain the reaction temperature at 25 °C during the experiment. Specifically, 0.035 g photocatalysts were ultrasonically dispersed in 70 mL of deionized water without any sacrificial agent. Before each measurement, the resulting mixture was degassed by bubbling  $\text{CO}_2$  for 30 min with stirring. The gas flow rate of  $\text{CO}_2$  was controlled at 7 mL  $\text{min}^{-1}$  by a mass flow controller (GFC17, Aalborg) throughout the photocatalytic process. A 300 Xe lamp with an AM 1.5G filter was used as the light source. The output light density was calibrated to 100 mW  $\text{cm}^{-2}$  using an optical power meter (Moletron POWER MAX 5200). The gas produced at different reaction times was detected and quantified online by a gas chromatograph (GC 9790Plus) equipped with a thermal conductivity detector (TCD) and a flame ionization detector (FID). Each  $\text{CO}_2$  reduction reaction experiment, including the control experiments, was repeated three times under the same conditions to ensure the reliability of the results. The average amounts of the products

and the standard deviations were calculated.  $^{13}\text{CO}_2$  was used as the feeding gas in the labeling experiment to confirm the origin of the generated products.

**Photoelectrochemical measurements.** The photoelectrochemical properties were carried out in 0.5 M  $\text{Na}_2\text{SO}_4$  electrolyte using a three-electrode electrochemical workstation (CHI-760E) at room temperature, which consists of a working electrode, reference electrode (Ag/AgCl) and counter electrode (Pt sheet). The working electrodes were prepared on fluorine-doped tin oxide (FTO) glass slides (coated area:  $1 \times 1 \text{ cm}^2$ ). 3 mg of the prepared samples were added to a mixture solution of ethanol (500  $\mu\text{L}$ ), water (500  $\mu\text{L}$ ), and Nafion (5 wt.%, 5  $\mu\text{L}$ ) to form a homogenous slurry through ultrasonication. Subsequently, the obtained slurry was spin-coated on a piece of pre-cleaned FTO collector and allowed to dry in a vacuum overnight at room temperature to obtain  $1 \times 1 \text{ cm}^2$  coating. The photoelectrodes were irradiated under simulated solar irradiation (AM 1.5G, 100  $\text{mW cm}^{-2}$ ). The photocurrents of the electrodes were measured using the amperometric (I-t curves) technique under repeatedly interrupted light irradiation. Mott-Schottky (M-S) plots were collected from -1 to 1 V under various frequencies (500 Hz, 1000 Hz, 1500 Hz) and 0.01 V amplitude. The electrochemical impedance spectroscopy (EIS) measurements were conducted under open-circuit potential with 0.01 to  $1 \times 10^5$  Hz frequency range and 0.005 V AC amplitude.

#### **In situ diffuse reflection infrared fourier transform spectroscopy (DRIFTS)**

**experiments.** DRIFTS measurements were conducted using the Bruker INVENIO R FT-IR spectrometer equipped with an in-situ diffuse reflectance cell (Harrick). Pure KBr powder was measured to obtain a background spectrum, and then the samples were mixed with KBr. During the measurement, the reaction cell was degassed by an ultrahigh vacuum pump and then purged with a dry Ar atmosphere for 30 min to sweep the impurities. The pure  $\text{CO}_2$  (99.999%) saturated by water vapor was then continually inlet into the specimen chamber. After 30 min adsorption equilibrium, the FTIR signals were collected after a certain irradiation duration. The spectra were obtained by subtracting the background from the spectra of the samples.

**Kelvin probe force microscopy measurements.** The Kelvin probe force microscope (KPFM) signals were detected by a SPA-400 (Seiko, Japan) atomic force microscope (AFM) instrument. The powder scraped off from the surface of photocatalysts had been pressed into a tablet (10 mm diameter, 1.5 mm thickness). Conductive Pt-coated silicon tips with a spring constant of 1-3 N/m and a tip radius of  $\sim 15 \text{ nm}$  (AC240-PP, Olympus, Japan) were used. KPFM equipped with light sources was employed to determine the light-induced variations in work function by measuring changes in contact potential difference (CPD).

**Computational details.** Spin-polarized density functional theory (DFT) calculations were performed by Vienna ab initio simulation package code (VASP) <sup>[1,2]</sup> with the projector augmented wave (PAW) method.<sup>[3]</sup> The electronic exchange-correlation function of the interacting electrons was treated using the Perdew-Burke-Ernzerhof (PBE) within the generalized gradient approximation (GGA).<sup>[4]</sup> The van der Waals interactions were described by the zero damping DFT-D3 method of Grimme scheme <sup>[5]</sup>. Cut-off energy of the plane-wave basis was set as 450 eV. For optimization of lattice size of Bi and Bi<sub>2</sub>O<sub>2</sub>CO<sub>3</sub> bulk structures, the Brillouin zone integration was performed with a Monkhorst-Pack<sup>5</sup> *k*-point sampling of 5×5×4 and 6×6×2, respectively. For optimization of geometry of Bi(100), Bi<sub>2</sub>O<sub>2</sub>CO<sub>3</sub>(100) and Bi(100)/Bi<sub>2</sub>O<sub>2</sub>CO<sub>3</sub>(100), the Brillouin zone integration was performed with a *k*-point sampling of 1×2×1. All the geometries were fully optimized until the atomic forces and energy were smaller than 0.02 eV Å<sup>-1</sup> and 10<sup>-5</sup> eV, respectively. Spin polarization method was introduced to describe magnetism of slab models. Charge density difference of Bi(100)/Bi<sub>2</sub>O<sub>2</sub>CO<sub>3</sub>(200) was set at 0.005 e Å<sup>-3</sup>. Density of states and work function of slab models were obtained by vaspkit interface.<sup>[6]</sup>

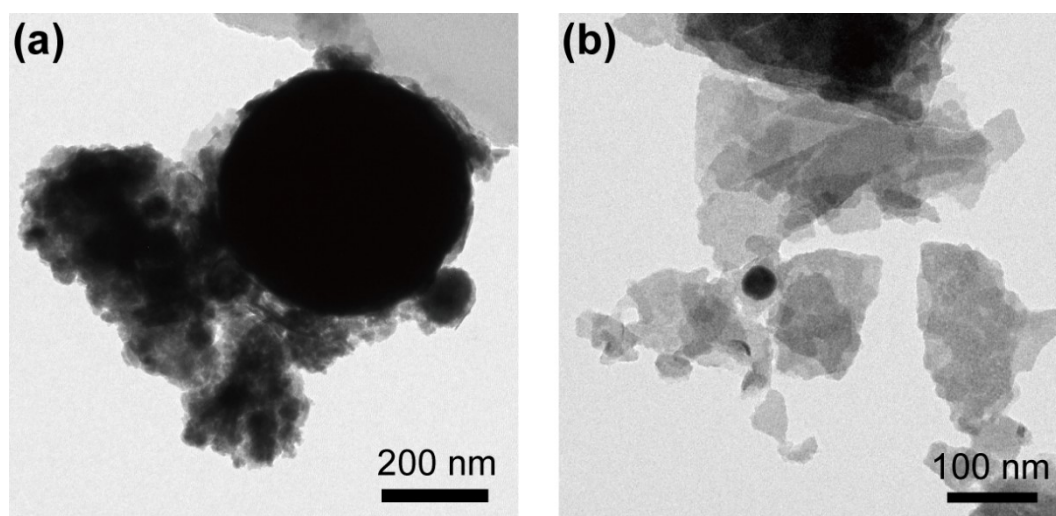


Fig. S1 TEM images of (a) DES Bi and (b) PEG Bi.

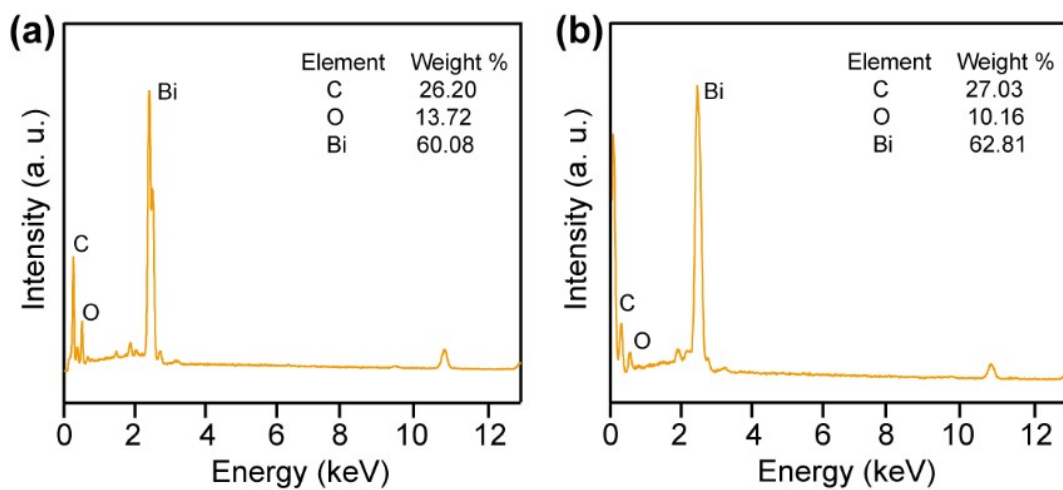


Fig. S2 EDS elemental analysis of (a) DES Bi and (b) PEG Bi.

The weight ratios of Bi, O, and C are almost the same in both samples. Therefore, the difference in photocatalytic performance can exclude the effect of elements.

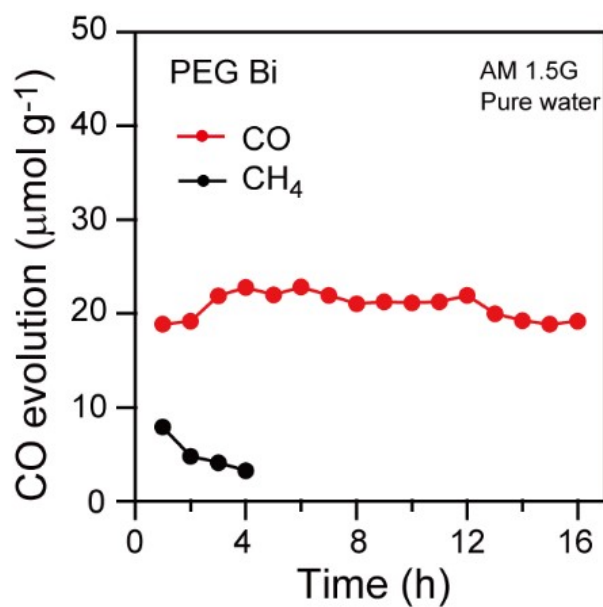


Fig. S3 Stability test over PEG Bi for 16 h reaction.

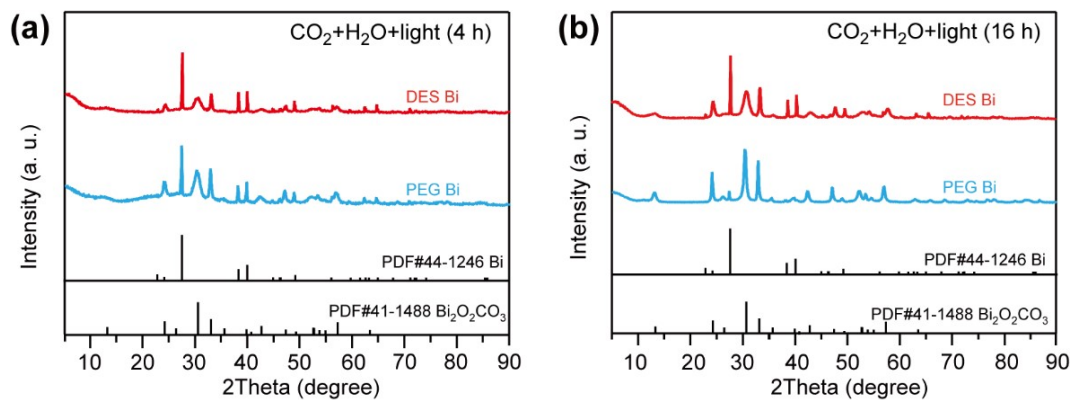


Fig. S4 XRD patterns of different samples after (a) 4 h and (b) 16 h reaction.

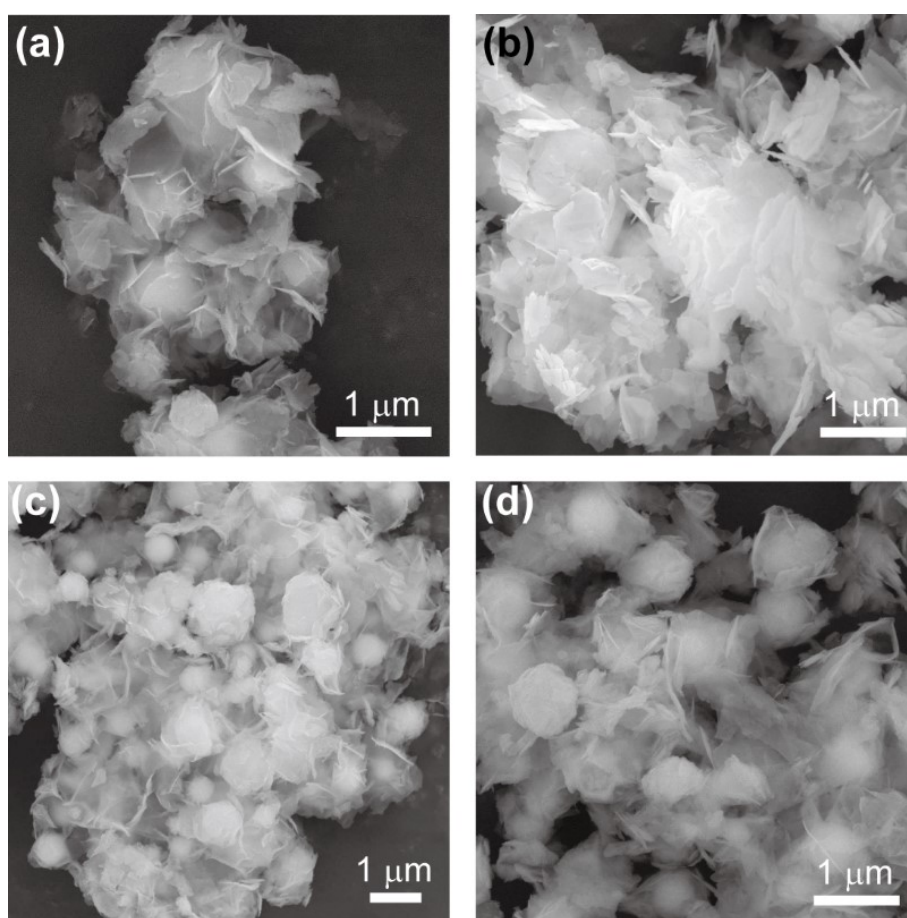


Fig. S5 SEM images of different samples after reaction. PEG Bi after (a) 4 h and (b) 16 h reaction. DES Bi after (c) 4 h and (d) 16 h reaction.

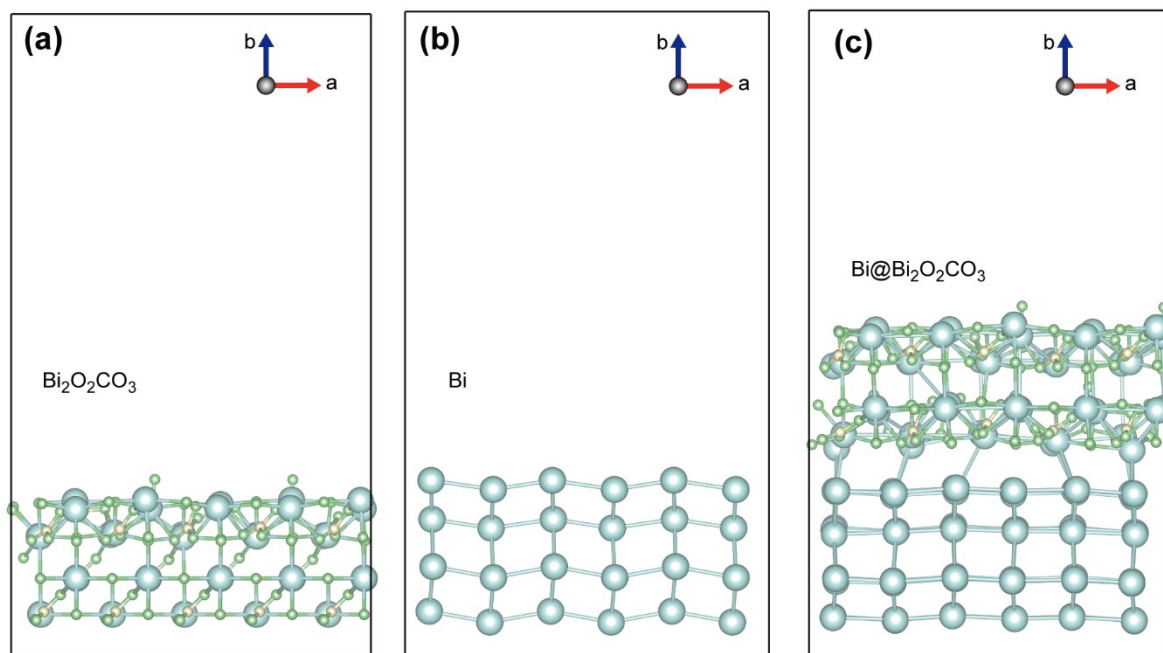


Fig. S6 (a, b) The simulated surface of  $\text{Bi}_2\text{O}_2\text{CO}_3$  (200) and Bi (100) plane. (c) optimized DFT calculations model of Bi (100)@ $\text{Bi}_2\text{O}_2\text{CO}_3$  (200) heterostructure.

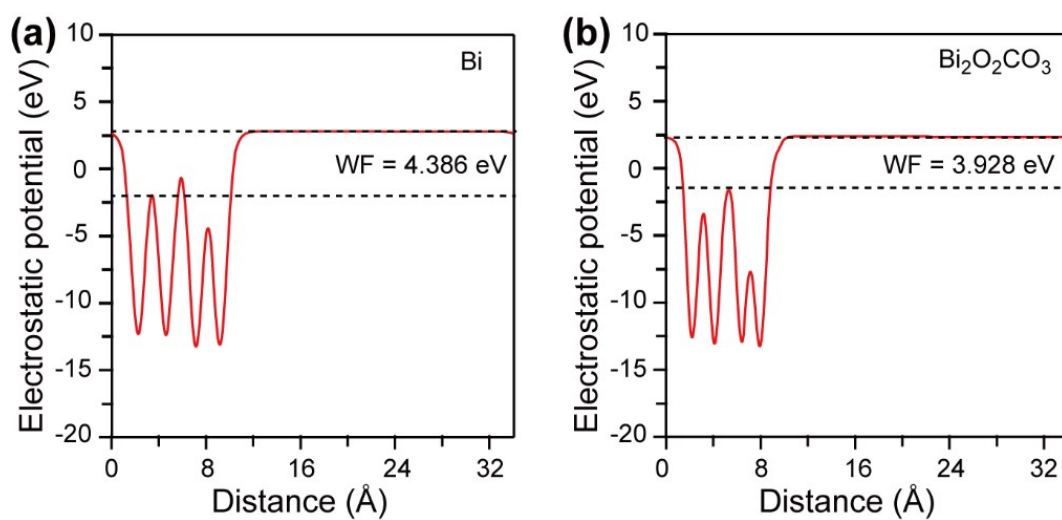


Fig. S7 The work functions of (a) Bi and (b)  $\text{Bi}_2\text{O}_2\text{CO}_3$ .



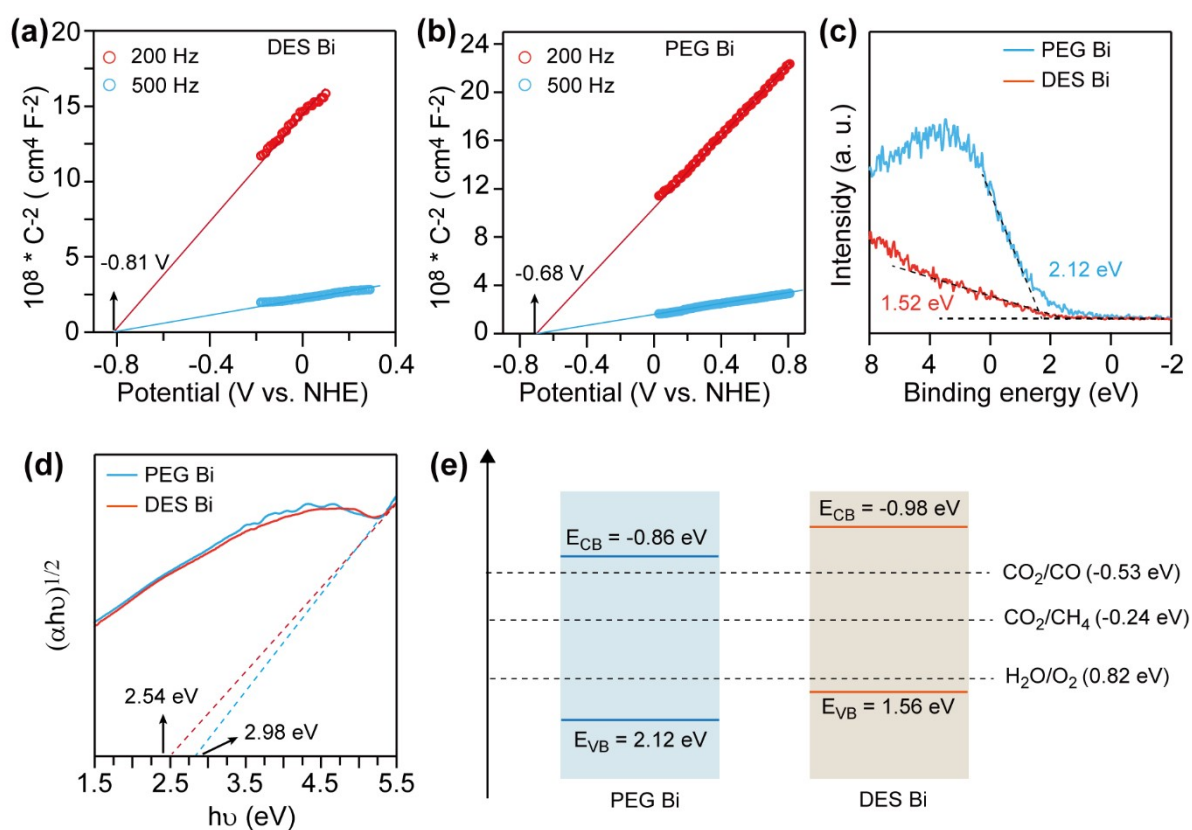


Fig. S8 Mott-Schottky plots of (a) PEG Bi and (b) DES Bi at different frequency; (c) Valence band XPS spectra; (d) Tauc plots; (e) Band structure alignments.

The positive slope observed in the M-S plots of all tested samples indicates that the DES Bi and PEG Bi exhibit n-type semiconductor characteristics. Based on the flat band potentials ( $E_{fb}$ ) and the reference values of the valence band in Fig. S8a-c, the valence band values ( $E_{VB}$ ) are calculated to be 2.12 and 1.56 eV, respectively. The conduction band values ( $E_{CB}$ ) can be calculated by subtracting the valence band values ( $E_{VB}$ ) from the  $E_g$  (Fig. S8d). The detailed band structure of DES Bi and PEG Bi are presented in Fig. S8e.

## References

- [1] Kresse, G., & Furthmüller, J. Efficient iterative schemes for ab initio total-energy calculations using a plane-wave basis set. *Phys. Rev. B*, 1996, **54**, 11169.
- [2] Kresse, G., & Furthmüller, J. Efficiency of ab-initio total energy calculations for metals and semiconductors using a plane-wave basis set. *Comput. Mater. Sci.*, 1996, **6**, 15-50.
- [3] Blöchl, P. E. Projector augmented-wave method. *Phys. Rev. B*, 1994, **50**, 17953.



- [4] Perdew, J. P., Burke, K., & Ernzerhof, M. Generalized gradient approximation made simple. *Phys. Rev. Lett.*, 1996, **77**, 3865.
- [5] Grimme, S., Ehrlich, S., & Goerigk, L. Effect of the damping function in dispersion corrected density functional theory. *J. Comput. Chem.*, 2011, **32**, 1456-1465.
- [6] Wang, V., Xu, N., Liu, J.-C., Tang, G., & Geng, W.-T. VASPKIT: A user-friendly interface facilitating high-throughput computing and analysis using VASP code. *Comput. Phys. Commun.*, 2021, **267**, 108033.